ACS APPLIED ENERGY MATERIALS

www.acsaem.org Letter

Instantaneous Surface Li_3PO_4 Coating and Al–Ti Doping and Their Effect on the Performance of $LiNi_{0.5}Mn_{1.5}O_4$ Cathode Materials

Valeriu Mereacre,* Nicole Bohn, Pirmin Stüble, Lukas Pfaffmann, and Joachim R. Binder

Cite This: *ACS Appl. Energy Mater.* 2021, 4, 4271–4276 Read Online

ACCESS | Metrics & More | Article Recommendations | Supporting Information

ABSTRACT: Using hydrogen peroxide (H_2O_2), a novel approach was applied for the synthesis of $LiNi_{0.5}Mn_{1.5}O_4$ (LNMO) coated with Li_3PO_4 and doped with Al^{3+} and Ti^{4+} ions. The reaction between LNMO and H_2O_2 resulted in particles with a partially damaged surface. If the same reaction is done in the presence of lithium, aluminum, titanium, and phosphate ingredients, then all particle facets are intact and show no sign of destruction. It appears that the H_2O_2 decomposition activates the LNMO surface, generating perfect conditions for the homogeneous deposition of the Li, Al, Ti, and phosphate ions. Electrochemical investigations show a very slow fading process during the cycling, and even after more than 500 cycles, the obtained cathode material shows a high specific capacity of 127 mAh g^{-1} (at 1 C) (~98% capacity retention) and an excellent Coulombic efficiency (99.5%).

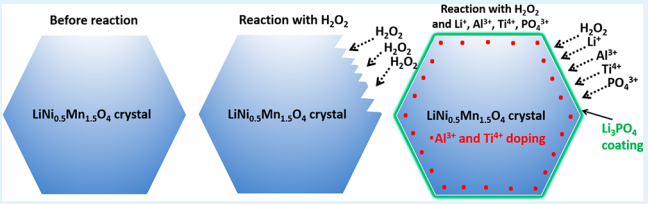

KEYWORDS: *Li_3PO_4 coating, cathode materials, lithium ion batteries, X-ray diffraction, electrochemistry*

Although spinel $LiNi_{0.5}Mn_{1.5}O_4$ (LNMO) could be used as an active material in high-power lithium ion batteries,[1−3] the unstable surface and interface characteristics are the main obstacles for its successful application. Usually, in the crystals of this kind of spinel, there is a minor amount of Mn^{3+} ions. Because of the disproportionation reaction of Mn^{3+}, the Mn^{2+} ions are obtained. These ions tend to dissolve into the electrolyte, and this process accelerates the capacity fade of the battery.[4−6] The most effective approach for protecting the LNMO particles is to avoid their direct contact with the electrolyte. This could be achieved by covering their surface with a protective layer.[7−10] The coating of cathode materials with $Li_{1.3}Al_{0.3}Ti_{1.7}(PO_4)_3$ (LATP) has been largely reported in the literature.[11−14] Generally, it is known that the conductivity of the $Li_{1+x}Al_xTi_{2-x}(PO_4)_3$ materials is related to their composition and the maximum stability for the $R\bar{3}c$ structure, and enhanced conductivity was observed for $x = 0.3$.[15]

An important approach for obtaining such coatings is essentially the same: a sol–gel method. While the reported studies have shown promising results for the ability of the obtained coatings to improve the electrochemical performance of the active materials, the direct observation of the coating chemistry and the coating structure and the full evidence of possible doping have not been shown. Furthermore, all studies have limited their investigation to bare and surface-modified cathodes, making the derivation of the real contribution of the coating difficult to assess. To obtain a crystalline coating layer with good ionic conductivity, the coated cathodic materials are exposed to a heat treatment. The thermal treatment not only will contribute to the synthesis and to crystallization of the coating material but also will influence the structure of the active material. Finally, the structural changes of the active material could be the reason for the improved electrochemical performance of the battery, but not the coating sample. Therefore, in order to identify the contributions from the coating process and composite in the coating layer, it is strongly recommended to produce a process reference compound. Such a material/uncoated sample exposed to the same thermal treatment as the coated one is useful for the reflection of the process influences.

The process of oxygen reduction into water is very important for many energy-conversion devices.[16−18] The possibility of using non-noble-metals as catalysts in such processes has stimulated a renewed attention of the scientists.[19,20] Recently, a series of studies showed strong activity of Mn oxides in the hydrogen peroxide reactions.[21] Being encouraged by these results, we decided to test the activity relative to hydrogen peroxide of one well-known cathode material, $LiNi_{0.5}Mn_{1.5}O_4$ oxide. A simple reaction between ~100 mg of LNMO and 10 mL of H_2O_2 resulted in a very violent reaction, which after approximately 1 min led to decomposition of H_2O_2. The XRD studies of the LNMO powder after the reaction have shown that the structure of LNMO has not changed. Although the LNMO (catalyst) seems to remain intact, during the reaction a large amount of heat is produced, which led us to conclude that the surface of

Received: January 18, 2021
Accepted: April 9, 2021
Published: April 22, 2021

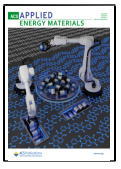

the catalyst for a short period of time becomes activated. It is expected that during the decomposition reaction the H_2O_2 adsorbate and LNMO adsorbent share electrons signifying the formation and/or breaking of chemical bonds. After the reaction and removal of H_2O and O_2 molecules from the surface of LNMO, these bonds are broken and shortly are free to mediate further reactions. Although the mechanism is not known (this is not the target of this study), we decided to use such a surface activation to obtain coated LNMO materials.

The goal of this work was the coating of the LNMO spinel particles with $Li_{1.3}Al_{0.3}Ti_{1.7}(PO_4)_3$, which is a kind of electrochemically stable inorganic material with high Li ion conductivity.[14] The composition and the concentration of the components in the solution used for the coating were considered accordingly. The pristine LNMO was synthesized by a coprecipitation method as previously reported.[22] The detailed synthesis of the pristine and coating materials is presented in the Supporting Information.

Although, even after the decomposition reaction presented above, the X-ray diffraction (XRD) patterns show no LNMO structure modifications, the scanning electron microscopy (SEM) studies show a partially damaged surface of the particles (Figure 1). What is curious is that mostly the (100)

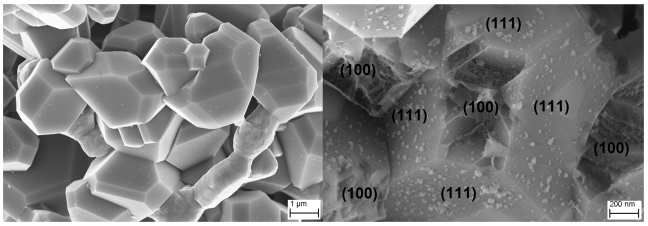

Figure 1. SEM diagrams of pristine LNMO (left) and LNMO treated with H_2O_2 (30%) (right).

facets of the truncated octahedral crystals were damaged. The reason for such behavior is not known, but it is believed to be related to factors such as cation ordering, oxygen vacancies, or size effects.

A brief look at the literature shows that truncated (100) facets might stabilize the spinel structure, support Li ion transport kinetics, and facilitate exceptional electrochemical performance for the LNMO cathode material.[23] If the same reaction is done in the presence of Li, Al, Ti, and phosphate ingredients, then the result is different: the particles show the same truncated octahedral microstructures with large portions of smooth and clean (100) facets, but the (100) facets are intact and show no sign of destruction (Figure 2). This indicates that the reaction of H_2O_2 with LNMO in the presence of the above-mentioned ingredients has not changed

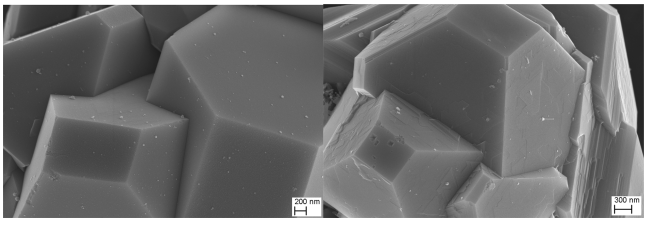

Figure 2. SEM diagrams of LNMO coated with 0.5 wt % Li–Al–Ti–PO_4 components and dried at 100 °C (left) and the same material calcined at 800 °C (right).

the micromorphology of the LNMO particles. It appears that the H_2O_2 decomposition activates the LNMO surface; generates "comfortable" conditions for the Li, Al, Ti, and phosphate ions to deposit homogeneously on the LNMO surface; and simultaneously protects it from further reaction with H_2O_2.

Due to the small quantity of the coating components, it is difficult to observe the presence of the coating layers at 100 °C (Figure 2, left). At 800 °C (Figure 2, right), however, well-distributed and overlapped crystalline multilayers are observed. Unfortunately, because of the concentration of the coating components being too small, in the XRD pattern only reflections typical for $LiNi_{0.5}Mn_{1.5}O_4$ are observed. A small shift of the diffraction reflections and a minor increase of the lattice parameters of the 0.5 wt % coated sample in comparison to the uncoated one, however, suggest a partial doping of the coated sample with Ti^{4+} ions. In order to confirm the results obtained by SEM and XRD analysis, XPS (X-ray photoelectron spectroscopy) analysis was also performed. Figure S3 shows XPS Mn 3s, Ni 3p, Al 2p, Ti 2p, and P 2p spectra of the uncoated (Figure S3, top) and coated LNMO (Figure S3, bottom) with 0.5 wt % Li–Al–Ti–PO_4 components. The 463.3 and 458.0 eV binding energies for Ti $2p_{1/2}$ and a Ti $2p_{3/2}$ spin–orbit separation of ~5.3 eV are usually observed for the Ti^{4+} ions in an octahedral oxygen environment.[24] The Al 2p peak at 76.0 eV is very weak, because of very small concentration of the Al ions in the coating layer. The P 2p spectrum displayed a peak at ~133.5 eV associated with the phosphate groups.[25]

To determine the possible structure of the composite coated on the surface, the same reaction was done with a bigger quantity of Li, Al, Ti, and phosphate components. The SEM images of the coated particles dried at 100 °C (Figure 3, left)

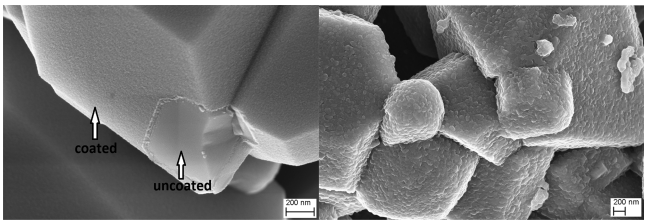

Figure 3. SEM diagrams of LNMO coated with 5 wt % Li–Al–Ti–PO_4 components and dried at 100 °C (left) and the same material calcined at 800 °C (right).

and calcined at 800 °C (Figure 3, right) demonstrate unquestionably the presence of a thick crystalline and very homogeneous coating layer. Taking into consideration the surface area of 0.3 $m^2\ g^{-1}$ for LNMO and theoretical density of LATP of 2.8 g cm^{-3}, a layer thickness of ~6 nm for the 0.5 wt % LATP and ~60 nm for the 5 wt % LATP-coated $LiMn_{1.5}Ni_{0.5}O_4$ particles could be assumed.

XRD was performed to detect the structural differences between the three above examined materials and one additional coated with 10 wt % (Figure 4): LNMO calcined at 800 °C (used as reference sample) and LNMO coated with 0.5, 5, and 10 wt %, and calcined at 800 °C. The XRD pattern of the 5 and 10 wt % samples calcined at 800 °C, in addition to the reflections typical for the spinel structure, shows several other weak reflections which confirm the presence of orthorhombic γ-Li_3PO_4[26] on the surface of LNMO particles but not of $Li_{1.3}Al_{0.3}Ti_{1.7}(PO_4)_3$. EDS studies (Figure S1) of the

https://doi.org/10.1021/acsaem.1c00160
ACS Appl. Energy Mater. 2021, 4, 4271–4276

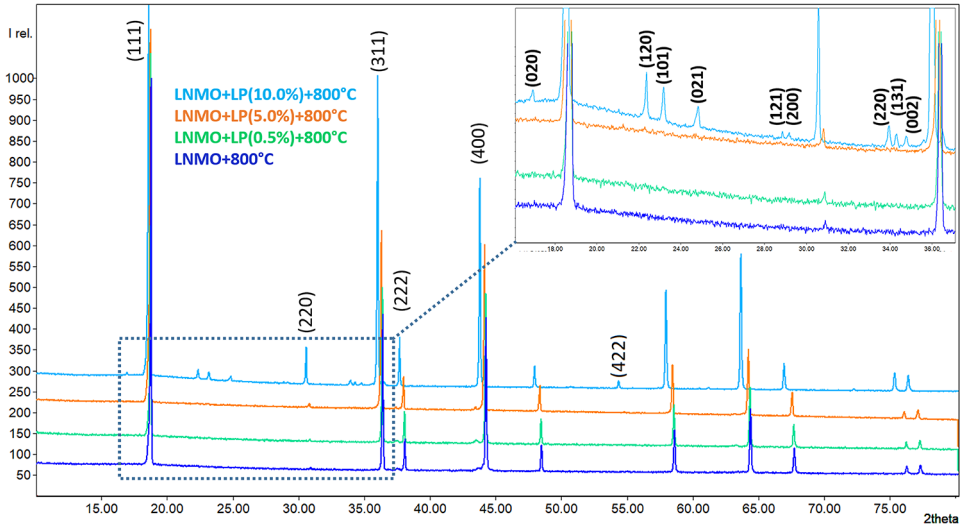

Figure 4. XRD patterns of uncoated $LiMn_{1.5}Ni_{0.5}O_4$ (LNMO) and coated with 0.5, 5, and 10 wt % coating material, and all four calcined at 800 °C. The reflections at 16.9°, 22.3°, 23.2°, 24.8°, 28.9°, 29.2°, 33.9°, 34.3°, and 34.8° correspond to coated Li_3PO_4. Inset: a zoomed 2θ region (16.0−37.0°) showing the Li_3PO_4 reflections.

5 wt % coated samples, on the other hand, also indicate the presence of Al and Ti ions in the coated samples. In general, the XRD patterns are similar for all three treated samples. However, there is one noticeable effect, which is easy to observe in the XRD patterns of the 10 wt % coated sample. The 220 and 422 reflections (~31° and ~54°) are a fingerprint for the occupation of the 8*a* tetrahedral site by heavy atoms.[27] In the case of LNMO + LP(10%) + 800 °C, they show much higher intensities, which is most likely due to partial Li substitution by Al^{3+} ions; Ti^{4+} ions in most of the cases tend to occupy the octahedral 16*d* sites.[28,29]

In order to better understand the individual properties of the diffraction patterns, Rietveld refinements were carried out using the Topas6 software. Due to strong X-ray absorption of the copper radiation, a uniform isotropic displacement parameter of B_{eq} of 0.5 had to be used. It must be assumed that phase fractions and the occupation factors in particular are subject to significant errors that exceed the values listed in Table S1. Nevertheless, refining the 8*a* Wyckoff position as a Li−Al mixed occupied site yields a ratio of 8 and 76% Al, separately, for the samples with 5 and 10 wt %. In contrast, refinement of the 0.5 wt % sample indicates pure Li occupation. The rocksalt secondary phase fraction was determined to be 3−4% in three of the four samples. The LNMO + LP(10%) + 800 °C sample hardly shows any rocksalt impurity phase. In contrast, the γ-Li_3PO_4 phase fraction was determined to 6.8%.

Another clear effect observed in the XRD patterns of 5 and 10 wt % coated samples is that they show an enlargement of the unit cell, also reflected by an obvious shift of the reflections toward smaller angles (Figure 4, inset; Table S1). The enlarged lattice parameters can be explained by partial substitution of Mn^{4+} (0.53 Å) ions with ions of a larger radius, in the present case, Ti^{4+} (0.605 Å). The shifts of the diffraction reflections and lattice parameters of the 0.5 wt % sample are smaller, due to a lower concentration of the Ti^{4+} doping ions in the structure. However, due to the similar structure factors of Ti, Mn, and Ni, a refinement of the Ti content on the 16*d* octahedral site was not possible.

It is known that Raman spectroscopy is sensitive to the crystal symmetry. In addition, it is a useful technique to identify the cation ordering. Figure S4 shows the Raman spectra of the uncoated and coated (5 wt %) LNMO powders, and both heat-treated at 800 °C. The peaks around 494 and 397 cm^{-1} are related to the Ni^{2+}−O stretching mode, whereas the peak at around 631 cm^{-1} is assigned to the symmetric Mn−O stretching modes.[30] A slight broadening of the Mn−O peak of the LNMO + LP(5%) + 800 °C sample most probably originates from partial doping with Ti ions. A nonsplit peak around 600 cm^{-1} is considered characteristic for disordered structures,[30] indicating that the coating process did not change the cation order degree of the uncoated material. The intense peak at approximately 970 cm^{-1} is attributed to the P−O vibrations in $\{PO_4\}$ tetrahedra.

In summary, using SEM, XPS, Raman, and XRD, it was possible to characterize the process of spinel coating and to identify the main component of the coating layer, γ-Li_3PO_4. Generally, if such a mixture of components, Li, Al, Ti, and phosphate, is used for the coating, the final substance that crystallized on the surface of the active cathode material is assumed to be LATP.[13,14] In order to isolate the pure LATP powder and to determine the possible structure of the phases, which could be synthesized by our new approach, the LATP precursor was prepared using the same components and the same heating process as that for the coated LNMO, but in the absence of LNMO. The XRD pattern of the obtained product is shown in Figure S2 and fits the structure of LATP. The coating processes with LATP are widely discussed in the literature, but no report demonstrates a clear structure of the LATP.[13,14] Our studies clearly reveal that the structure of the coating material, no matter which concentration is in use, corresponds not to LATP but to Li_3PO_4, and Al^{3+} and Ti^{4+} ions are consumed for doping of the active material. Even when the concentration of the coating components is ~10 wt %, the structure of the final coating material still matches that of Li_3PO_4 (Figure 4, inset).

It should be mentioned that there are only several examples of Li_3PO_4-coated spinel cathode materials reported so far.[31−33] Kobayashi et al. used Li_3PO_4-coated LNMO to prevent the

https://doi.org/10.1021/acsaem.1c00160
ACS Appl. Energy Mater. 2021, 4, 4271−4276

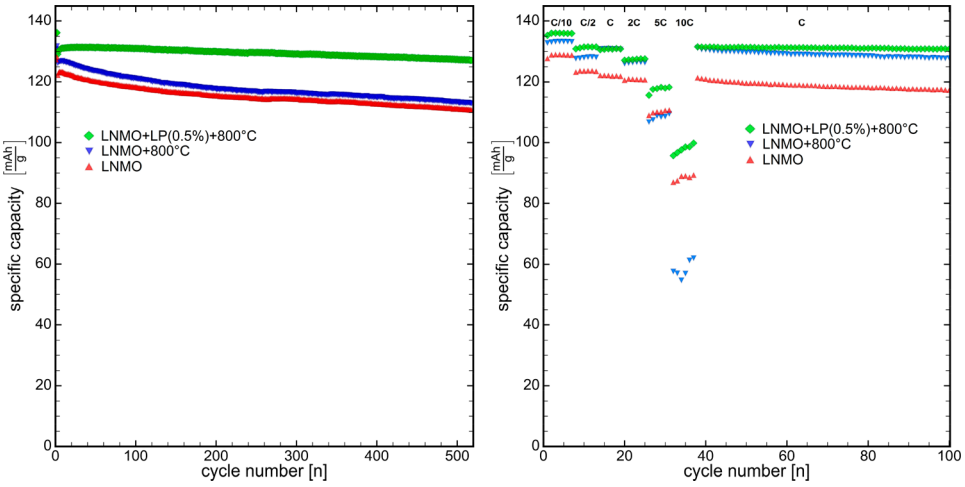

Figure 5. (Left) Capacity retention test at charge−discharge rate of C/2 − C and (right) rate capability test of the three samples: LNMO, LNMO + 800 °C, and LNMO + LP(0.5%) + 800 °C.

degradation of solid polymer electrolyte in an all-solid-state lithium battery.[31] In order to study the contribution of the surface bridging ions to the establishment of stronger bonds between the spinel and Li_3PO_4, using a hydrothermal method, Huang et al. synthesized a Li_3PO_4-coated LNMO.[32] Since solid electrolytes are more stable at a high operating voltage than organic liquid electrolytes, using pulsed laser deposition (PLD), a Li_3PO_4-coated LNMO material was also prepared and tested as a positive electrode in the all-solid-state batteries with $Li_2S-P_2S_5$ as solid electrolyte.[33]

To explore how the structural and morphological changes influences the electrochemical activity of the coated LNMO spinel obtained in this work, the cycle-life performances of bare LNMO, LNMO calcined at 800 °C (reference compound), and LNMO 0.5 wt % coated and calcined at 800 °C were tested and compared. The choice of 800 °C as the temperature was based on the published results, which show that at this temperature LNMO has a $Fd\bar{3}m$ space group and displays a high discharge capacity and the best cycling performance.[34−36] The electrochemical data for the 5 and 10 wt % coated samples are not illustrative, because the coating layer of these samples is very thick and forms a barrier for the movement of lithium ions. In addition, the low ionic conductivity of the Li_3PO_4 ($\sim 10^{-18}$ S cm^{-1}) plays its negative role.[37,38] The details about electrochemical measurements are presented in the Supporting Information.

The long-term cycling performance of the three materials mentioned above is shown in Figure 5, left. The cells were initially charged−discharged for two cycles at 0.1 C, and then charged (at 0.5 C) and discharged (at 1 C) for more than 500 times with the voltage of 3.5−5.0 V. The Coulombic efficiency of all electrodes was ∼99.5% at the charge−discharge cycle, which indicates a very high reversibility of the composite electrodes. The pristine LNMO and LNMO + 800 °C display initial capacities of ∼123.2 and 126.9 mAh g^{-1}, respectively. However, both electrodes show a comparable degree of capacity fading: after 500 cycles, the remaining capacity for the original LNMO is 90.2%, and for the calcined LNMO + 800 °C, it is 89.1%. On the other hand, the coated sample LNMO + LP(0.5%) + 800 °C shows not only a higher initial capacity (∼132.0 mAh g^{-1}) but also a higher stability and capacity retention (∼97.8%).

In order to characterize the process of Li ion migration, the rate capability was tested. This test was performed as previously reported:[22] at the potential range of 3.5−5.0 V and different scan rates of 0.1, 0.5, 1, 2, 5, 10 C (Figure 5, right). If the discharge rate of the bare LNMO material is increased from 0.1 to 10 C, then its discharge capacity shows a reduction from 128.8 to 88.8 mAh g^{-1}. Such a decrease corresponds to 69.0% capacity retention. Two other materials, LNMO + 800 °C and LNMO + LP(0.5%) + 800 °C, show 45.0% (from 133.6 to 58.8 mAh g^{-1}) and 72.0% (from 136.2 to 98.1 mAh g^{-1}) capacity retentions, respectively. Therefore, one can conclude that the rate capability of the LNMO material gets worse if an extra thermal treatment at 800 °C is performed, but if the same sample is coated and treated at 800 °C, then a higher capacity retention at high cycling rates is obtained. Hence, the pure contribution of the coating and doping is obvious.

Interestingly, once the LNMO + 800 °C cell is cycled at high rates and the current density proceeds back to 1 C, it recuperates its initial capacity which is similar to the capacity of the LNMO + LP(0.5%) + 800 °C electrode. It seems that, after cycling at high rates, the structure of the pristine material additionally calcined at 800 °C undergoes certain changes, which favor a better Li ion intercalation and, respectively, an enhanced performance. Unfortunately, further cycling shows a faster fading for LNMO + 800 °C in comparison to LNMO + LP(0.5%) + 800 °C (Figure 5, right, and Figure S5), which again indicates the positive contribution of the coating process on the stability of the active material. It should be mentioned that the discharge capacity of the LNMO + 800 °C sample at 1 C is slightly higher than at C/2 (Figure 5, right). Such a phenomenon is not new, and it is suggested that the wetting and activation process of this sample needed a slightly longer time, and as a result, a larger capacity is obtained later.[23,39]

Another remarkable observation, which also points to the positive input of the coating, was made from differential capacity versus potential (dQ/dV) curves (Figure S6). Figure S7 shows the dQ/dV curves for the Ni^{3+}/Ni^{4+} redox couple extracted from the capacity retention test for the range between the 5th and 100th cycles. All of the peaks, regardless of the sample being the original or the temperature- or Li_3PO_4-modified spinel, show a similar shape, but the polarization of the coated material between the fifth and the 100th cycle is

https://doi.org/10.1021/acsaem.1c00160
ACS Appl. Energy Mater. 2021, 4, 4271−4276

obviously decreasing compared to those of the uncoated and reference samples. If, for example, we analyze the oxidation peaks caused by the Ni^{3+}/Ni^{4+} redox couple for LNMO and LNMO + 800 °C, they shift from 4.767 and 4.776 V in the 5th cycle to 4.769 and 4.779 V after the 100th cycle, respectively. As a comparison, the corresponding oxidation peak shift of the coated sample is larger and with the opposite sign (−) from 4.777 to 4.773 V.

In summary, a new coating process was developed, allowing surface activation and simultaneous coating and doping. This was possible due to the property of manganese oxides to catalyze the decomposition of hydrogen peroxide. The coated LNMO exhibits higher capacity, cycling stability, and rate capability, and lower polarization than the pristine and reference samples. Its capacity retention is ∼98% after 500 cycles and is higher than that of the pristine material (∼90%). In addition, it shows a superior rate capability with a capacity of 98 mAh g^{-1} at 10 C, while for the pristine it is only 89 mAh g^{-1}. It was also concluded that the reference compounds are very important for distinguishing between the influence of the process and the effect of composite present in the coating system.

Even though the benefits of the Li_3PO_4 coating for LNMO are notable, further analysis is planned to determine the nature of the formed phases at lower temperatures, for example, at 500 °C, when the doping did not take place yet and the possible structure of the coating material corresponds to an amorphous LATP. Also, neutron diffraction analysis and transmission electron microscopy are scheduled to confirm the structure of extra phases that may have formed in the LNMO + LP(0.5%) + 800 °C sample and to determine the state of the spinel structure in coated and uncoated materials after cycling. Such studies will be offered in a future publication.

■ ASSOCIATED CONTENT

Supporting Information

The Supporting Information is available free of charge at https://pubs.acs.org/doi/10.1021/acsaem.1c00160.

Experimental methods details; EDS, Raman, and XPS images; XRD results; additional electrochemical data; and results of the Rietveld refinement (PDF)

■ AUTHOR INFORMATION

Corresponding Author

Valeriu Mereacre − *Institute for Applied Materials—Energy Storage Systems, Karlsruhe Institute of Technology, D-76344 Eggenstein-Leopoldshafen, Germany;* orcid.org/0000-0002-8295-6078; Email: valeriu.mereacre@kit.edu

Authors

Nicole Bohn − *Institute for Applied Materials—Energy Storage Systems, Karlsruhe Institute of Technology, D-76344 Eggenstein-Leopoldshafen, Germany*

Pirmin Stüble − *Institute for Applied Materials—Energy Storage Systems, Karlsruhe Institute of Technology, D-76344 Eggenstein-Leopoldshafen, Germany; Helmholtz Institute Ulm, D-89081 Ulm, Germany*

Lukas Pfaffmann − *Institute for Applied Materials—Energy Storage Systems, Karlsruhe Institute of Technology, D-76344 Eggenstein-Leopoldshafen, Germany*

Joachim R. Binder − *Institute for Applied Materials—Energy Storage Systems, Karlsruhe Institute of Technology, D-76344 Eggenstein-Leopoldshafen, Germany;* orcid.org/0000-0003-2237-1411

Complete contact information is available at: https://pubs.acs.org/10.1021/acsaem.1c00160

Author Contributions

All authors have given approval to the final version of the manuscript.

Notes

The authors declare no competing financial interest.

■ ACKNOWLEDGMENTS

This work was carried out with the support of the Helmholtz Energy Materials Foundry (HEMF), a large-scale distributed research infrastructure founded by the German Helmholtz Association. It also contributes to the research performed at CELEST (Center for Electrochemical Energy Storage Ulm-Karlsruhe).

■ REFERENCES

(1) Santhanam, R.; Rambabu, B. Research Progress in High Voltage Spinel $LiNi_{0.5}Mn_{1.5}O_4$ Material. *J. Power Sources* **2010**, *195*, 5442−5451.

(2) Patoux, S.; Daniel, L.; Bourbon, C.; Lignier, H.; Pagano, C.; Le Cras, F.; Jouanneau, S.; Martinet, S. High Voltage Spinel Oxides for Li-ion batteries: From the Material Research to the Application. *J. Power Sources* **2009**, *189*, 344−352.

(3) Kunduraci, M.; Al-Sharab, J. F.; Amatucci, G. G. High-Power Nanostructured $LiMn_{2-x}Ni_xO_4$ High-Voltage Lithium-Ion Battery Electrode Materials: Electrochemical Impact of Electronic Conductivity and Morphology. *Chem. Mater.* **2006**, *18*, 3585−3592.

(4) Sun, Y. K.; Hong, K. J.; Prakash, J.; Amine, K. Electrochemical Performance of Nano-Sized ZnO-Coated $LiNi_{0.5}Mn_{1.5}O_4$ Spinel as 5 V Materials at Elevated Temperatures. *Electrochem. Commun.* **2002**, *4*, 344−348.

(5) Talyosef, Y.; Markovsky, B.; Salitra, G.; Aurbach, D.; Kim, H. J.; Choi, S. The Study of $LiNi_{0.5}Mn_{1.5}O_4$ 5 V Cathodes for Li-Ion Batteries. *J. Power Sources* **2005**, *146*, 664−669.

(6) Markovsky, B.; Talyossef, Y.; Salitra, G.; Aurbach, D.; Kim, H. J.; Choi, S. Cycling and Storage Performance at Elevated Temperatures of $LiNi_{0.5}Mn_{1.5}O_4$ Positive Electrodes for Advanced 5 V Li-ion Batteries. *Electrochem. Commun.* **2004**, *6*, 821−826.

(7) Shim, J.; Lee, S.; Park, S. Effects of MgO Coating on the Structural and Electrochemical Characteristics of $LiCoO_2$ as Cathode Materials for Lithium Ion Battery. *Chem. Mater.* **2014**, *26*, 2537−2543.

(8) Kim, M. G.; Cho, J. Air Stable Al_2O_3-Coated Li_2NiO_2 Cathode Additive as a Surplus Current Consumer in a Li-Ion Cell. *J. Mater. Chem.* **2008**, *18*, 5880−5887.

(9) Wang, J.-H.; Wang, Y.; Guo, Y.-Z.; Ren, Z.-Y.; Liu, C.-W. Effect of Heat-Treatment on the Surface Structure and Electrochemical Behavior of $AlPO_4$-Coated $LiNi_{1/3}Co_{1/3}Mn_{1/3}O_2$ Cathode Materials. *J. Mater. Chem. A* **2013**, *1*, 4879−4884.

(10) Huang, B.; Li, X.; Wang, Z.; Guo, H.; Shen, L.; Wang, J. A Comprehensive Study on Electrochemical Performance of Mn-Surface-Modified $LiNi_{0.8}Co_{0.15}Al_{0.05}O_2$ Synthesized by an in Situ Oxidizing-Coating Method. *J. Power Sources* **2014**, *252*, 200−207.

(11) Liu, Y.; Fan, X.; Huang, X.; Liu, D.; Dou, A.; Su, M.; Chu, D. Electrochemical Performance of $Li_{1.2}Ni_{0.2}Mn_{0.6}O_2$ Coated with a Facilely Synthesized $Li_{1.3}Al_{0.3}Ti_{1.7}(PO_4)_3$. *J. Power Sources* **2018**, *403*, 27−37.

(12) Wang, Y.; Liu, B.-N.; Zhou, G.; Nie, K.-H.; Zhang, J.-N.; Yu, X.-Q.; Li, H. Improved Electrochemical Performance of Li-

$(Ni_{0.6}Co_{0.2}Mn_{0.2})O_2$ at High Charging Cut-off Voltage with $Li_{1.4}Al_{0.4}Ti_{1.6}(PO_4)_3$ Surface Coating. *Chin. Phys. B* **2019**, *28*, 068202.
(13) Wang, T.; Yang, Z.; Jiang, Y.; Li, G.; Huang, Y. Improving the Electrochemical Performance of $Li_{1.2}Ni_{0.13}Co_{0.13}Mn_{0.54}O_2$ by Li-ion Conductor. *RSC Adv.* **2016**, *6*, 63749−63753.
(14) Deng, Y.-F.; Zhao, S.-X.; Xu, Y.-H.; Nan, C.-W. Effect of Temperature of $Li_2O-Al_2O_3-TiO_2-P_2O_5$ Solid-State Electrolyte Coating Process on the Performance of $LiNi_{0.5}Mn_{1.5}O_4$ Cathode Materials. *J. Power Sources* **2015**, *296*, 261−267.
(15) Aono, H.; Sugimoto, E.; Sadaoka, Y.; Imanaka, N.; Adachi, G.-y. Ionic Conductivity of the Lithium Titanium Phosphate $(Li_{1+x}M_xTi_{2-x}(PO_4)_3$ M = Al, Sc, Y, and La) Systems. *J. Electrochem. Soc.* **1989**, *136*, 590−591.
(16) Zhang, Z.; Liu, J.; Gu, J.; Su, L.; Cheng, L. An Overview of Metal Oxide Materials as Electrocatalysts and Supports for Polymer Electrolyte Fuel Cells. *Energy Environ. Sci.* **2014**, *7*, 2535−2558.
(17) Cheng, F.; Chen, J. Metal−Air Batteries: from Oxygen Reduction Electrochemistry to Cathode Catalysts. *Chem. Soc. Rev.* **2012**, *41*, 2172−2192.
(18) Desmond Ng, J. W.; Gorlin, Y.; Hatsukade, T.; Jaramillo, T. F. A Precious-Metal-Free Regenerative Fuel Cell for Storing Renewable Electricity. *Adv. Energy Mater.* **2013**, *3*, 1545−1550.
(19) Hong, W. T.; Risch, M.; Stoerzinger, K. A.; Grimaud, A.; Suntivich, J.; Shao-Horn, Y. Toward the Rational Design of Non-Precious Transition Metal Oxides for Oxygen Electrocatalysis. *Energy Environ. Sci.* **2015**, *8*, 1404−1427.
(20) He, Q.; Cairns, E. J. Review—Recent Progress in Electrocatalysts for Oxygen Reduction Suitable for Alkaline Anion Exchange Membrane Fuel Cells. *J. Electrochem. Soc.* **2015**, *162*, F1504−F1539.
(21) Ryabova, A. S.; Bonnefont, A.; Zagrebin, P.; Poux, T.; Paria Sena, R.; Hadermann, J.; Abakumov, A. M.; Kerangueven, G.; Istomin, S. Y.; Antipov, E. V.; Tsirlina, G. A.; Savinova, E. R. Study of Hydrogen Peroxide Reactions on Manganese Oxides as a Tool To Decode the Oxygen Reduction Reaction Mechanism. *ChemElectroChem* **2016**, *3*, 1667−1677.
(22) Mereacre, V.; Bohn, N.; Müller, M.; Indris, S.; Bergfeldt, T.; Binder, J. R. Improved Performance of High-Voltage Li-Ion Batteries Using a Novel Chemically Activated Coating Process. *Mater. Res. Bull.* **2021**, *134*, 111095.
(23) Liu, H.; Kloepsch, R.; Wang, J.; Winter, M.; Li, J. Truncated Octahedral $LiNi_{0.5}Mn_{1.5}O_4$ Cathode Material for Ultralong Life Lithium-Ion Battery: Positive (100) Surfaces in High-Voltage Spinel System. *J. Power Sources* **2015**, *300*, 430−437.
(24) Zheng, J.; Liu, Y. S.; Ji, G. B.; Zhang, P.; Cao, X. Z.; Wang, B. Y.; Zhang, C. H.; Zhou, X. G.; Zhu, Y.; Shi, D. N. Hydrogenated Oxygen Deficient Blue Anatase as Anode for High Performance Lithium Batteries. *ACS Appl. Mater. Interfaces* **2015**, *7*, 23431−23438.
(25) Qiao, Q. Q.; Zhang, H. Z.; Li, G. R.; Ye, S. H.; Wang, C. W.; Gao, X. P. Surface Modification of Li-Rich Layered Li-$(Li_{0.17}Ni_{0.25}Mn_{0.58})O_2$ Oxide with Li-Mn-PO_4 as the Cathode for Lithium-Ion Batteries. *J. Mater. Chem. A* **2013**, *1*, 5262−5268.
(26) Bondareva, O. S. The Crystal Structure of the Synthetic Analogue of the Lithiophospate Li_3PO_4-Gamma. *Dokl. Akad. Nauk SSSR* **1978**, *240*, 75−77.
(27) Le, M.-L.-P.; Strobel, P.; Colin, C. V.; Pagnier, T.; Alloin, F. Spinel-Type Solid Solutions Involving Mn^{4+} and Ti^{4+}:Crystal Chemistry, Magnetic and Electrochemical Properties. *J. Phys. Chem. Solids* **2011**, *72*, 124−135.
(28) Arrebola, J. C.; Caballero, A.; Cruz, M.; Hernan, L.; Morales, J.; Castellon, E. R. Crystallinity Control of a Nanostructured $LiNi_{0.5}Mn_{1.5}O_4$ Spinel via Polymer-Assisted Synthesis: A Method for Improving Its Rate Capability and Performance in 5 V Lithium Batteries. *Adv. Funct. Mater.* **2006**, *16*, 1904−1912.
(29) Shin, D. W.; Bridges, C. A.; Huq, A.; Paranthaman, M. P.; Manthiram, A. Role of Cation Ordering and Surface Segregation in High-Voltage Spinel $LiMn_{1.5}Ni_{0.5-x}M_xO_4$ (M = Cr, Fe, and Ga) Cathodes for Lithium-Ion Batteries. *Chem. Mater.* **2012**, *24*, 3720−3731.
(30) Amdouni, N.; Zaghib, K.; Gendron, F.; Mauger, A.; Julien, C. M. Structure and Insertion Properties of Disordered and Ordered $LiNi_{0.5}Mn_{1.5}O_4$ Spinels Prepared by Wet Chemistry. *Ionics* **2006**, *12*, 117−126.
(31) Kobayashi, Y.; Miyashiro, H.; Takei, K.; Shigemura, H.; Tabuchi, M.; Kageyama, H.; Iwahori, T. 5 V Class All-Solid-State Composite Lithium Battery with Li_3PO_4 Coated $LiNi_{0.5}Mn_{1.5}O_4$. *J. Electrochem. Soc.* **2003**, *150*, A1577−A1582.
(32) Wu, Y.; Ben, L.; Yu, H.; Qi, W.; Zhan, Y.; Zhao, W.; Huang, X. Understanding the Effect of Atomic-Scale Surface Migration of Bridging Ions in Binding Li_3PO_4 to the Surface of Spinel Cathode Materials. *ACS Appl. Mater. Interfaces* **2019**, *11*, 6937−6947.
(33) Yubuchi, S.; Ito, Y.; Matsuyama, T.; Hayashi, A.; Tatsumisago, M. 5 V Class $LiNi_{0.5}Mn_{1.5}O_4$ Positive Electrode Coated with Li_3PO_4 Thin Film for All-Solid-State Batteries Using Sulfide Solid Electrolyte. *Solid State Ionics* **2016**, *285*, 79−82.
(34) Kim, J.-H.; Myung, S.-T.; Yoon, C. S.; Kang, S. G.; Sun, Y.-K. Comparative Study of $LiNi_{0.5}Mn_{1.5}O_{4-\delta}$ and $LiNi_{0.5}Mn_{1.5}O_4$ Cathodes Having Two Crystallographic Structures: $F_{d\bar{3}m}$ and P_{4332}. *Chem. Mater.* **2004**, *16*, 906−914.
(35) Lee, E.; Persson, K. A. Revealing the Coupled Cation Interactions Behind the Electrochemical Profile of $Li_xNi_{0.5}Mn_{1.5}O_4$. *Energy Environ. Sci.* **2012**, *5*, 6047−6051.
(36) Kunduraci, M.; Amatucci, G. G. Effect of Oxygen Non-Stoichiometry and Temperature on Cation Ordering in $LiMn_{2-x}Ni_xO_4(0.50 \geq x \geq 0.36)$ Spinels. *J. Power Sources* **2007**, *165*, 359−367.
(37) Gaur, K.; Pathak, A.; Lal, H. Ionic and Electronic Conductivity in Some Simple Lithium Salts. *J. Mater. Sci.* **1988**, *23*, 4257−4262.
(38) Lee, C.; Dutta, P. K.; Ramamoorthy, R.; Akbar, S. A. Mixed Ionic and Electronic Conduction in Li_3PO_4 Electrolyte for a CO_2 Gas Sensor. *J. Electrochem. Soc.* **2006**, *153*, H4−H14.
(39) Zhou, L.; Zhao, D.; Lou, X. D. $LiNi_{0.5}Mn_{1.5}O_4$ Hollow Structures as High-Performance Cathodes for Lithium-Ion Batteries. *Angew. Chem., Int. Ed.* **2012**, *51*, 239−241.

https://doi.org/10.1021/acsaem.1c00160
ACS Appl. Energy Mater. 2021, 4, 4271−4276